Results in Physics 14 (2019) 102440

Contents lists available at ScienceDirect

Results in Physics

journal homepage: www.elsevier.com/locate/rinp

Effects of annealing on the structures and properties of Er,Yb:$LuGdVO_4$ crystal

Nianjing Ji[a,c], Yang Chen[a], Ziqing Li[a], Jiyang Wang[a], Xiulan Duan[a,*], Kegao Liu[c], Huaidong Jiang[a,b,*]

[a] State Key Laboratory of Crystal Materials, Institute of Crystal Materials, Shandong University, Jinan 250100, China
[b] School of Physical Science and Technology, ShanghaiTech University, Shanghai 201210, China
[c] School of Materials Science and Engineering, Shandong Jianzhu University, Fengming Road, Jinan 250101, China

ARTICLE INFO

Keywords:
Er,Yb:$LuGdVO_4$
Annealing
XPS
Optical property

ABSTRACT

The Er,Yb:$LuGdVO_4$ crystal was grown by the Czochralski method under the oxygen-deficient atmosphere, and cut into slices, which were annealed in different conditions. The crystalline quality of the as-grown crystal was characterized by high resolution X-ray diffraction (HRXRD). The effects of different annealing conditions on the structures, chemical states and local symmetry of Er,Yb:$LuGdVO_4$ were studied by X-ray diffraction (XRD), Raman, X-ray photoelectron spectroscopy (XPS) and X-ray absorption near edge structure (XANES) in detail. The content of V^{4+} in the crystal obviously decreased after annealing. The distribution of elements in the sample was analyzed by the SR-based X-ray fluorescence (XRF). The specific heat and thermal diffusion of Er,Yb:$LuGdVO_4$ crystal were measured, and absorption spectra of the samples annealed in different conditions were recorded at room temperature. The results show that the annealing process has few influences on the thermal properties and remarkable influences on the optical properties.

Introduction

As laser host media for Nd, Yb and Er ions, orthovanadate crystals including YVO_4, $GdVO_4$ and $LuVO_4$, and their mixed vanadate crystals such as $Gd_xY_{1-x}VO_4$, $Y_xLu_{1-x}VO_4$, and $Lu_xGd_{1-x}VO_4$ have attracted much attention of the researchers working on solid-state lasers [1–3]. The $LuGdVO_4$ owns as good thermal property as YVO_4. A great deal of attention has been focused on Er, Yb co-dope $LuGdVO_4$, which possesses a good application prospect for eye-safe 1.5 μm lasers. The researches mainly focus on the thermal, optical and laser performance of the vanadate crystals. Until now, there are few reports on the microstructure research of the mixed vanadate crystals.

Czochralski is one of the popular method to grow large vanadate crystals. In the Czochralski crystal growth process, the crystal defects are generally caused by the atmosphere and high speed cooling rate in the growth and cooling process. The oxygen-deficient atmosphere can reduce the oxide impurities and protect equipment. So the crystals are usually fabricated under low oxygen atmosphere such as $N_2 + O_2$ (2 vol %) [4]. The high quality Er^{3+}:$GdVO_4$ was grown in N_2 atmosphere, and then annealed under the atmosphere 3–5 vol% O_2 after the melt surface frozen in the cooling process [5]. There are amount of oxygen vacancies in the crystal due to the oxygen-deficient atmosphere in the growth and cooling process. All the crystals have to be annealed in the air at high temperature before cutting, which can reduce the defects such as oxygen vacancies and dislocations. We find that the color of Er,Yb:$LuGdVO_4$ changes obviously after the second annealing. So the crystal color is not only related to the change of doping amount, but also to the annealing process, It may be attributed to the color center disappearing in the annealing process, which shows a serious impact on the optical properties of the crystal.

The current work is focused on comparative study of Er,Yb:$LuGdVO_4$ crystal grown in N_2 atmosphere and annealed in different conditions. The effects of different annealing conditions on the structures and properties of Er,Yb:$LuGdVO_4$ were studied by XRD, XRF, XPS, XANES, Raman, SR-based XRF etc.

Experimental

Raw materials RVO_4 (R = Yb, Er, Lu, Gd) with 99.99% purity were used to grow the $Er_{0.01}$, $Yb_{0.02}$:$Lu_{0.485}Gd_{0.485}VO_4$ in stoichiometric. The Er,Yb:$LuGdVO_4$ crystal was grown by Czochralski method with a radio frequency heating furnace in N_2 atmosphere. The detailed growth process was described in Ref. [6,7]. At the end of growth, the crystal was rapidly cooled down to room temperature. Due to oxygen-deficient

* Corresponding authors at: State Key Laboratory of Crystal Materials, Institute of Crystal Materials, Shandong University, Jinan 250100, China.
E-mail addresses: xlduan@sdu.edu.cn (X. Duan), jianghd@sdu.edu.cn, jianghd@shanghaitech.edu.cn (H. Jiang).

https://doi.org/10.1016/j.rinp.2019.102440
Received 22 April 2019; Received in revised form 31 May 2019; Accepted 11 June 2019
Available online 15 June 2019

Table 1
Different annealing conditions for Er,Yb:LuGdVO$_4$.

Sample	T/°C	Time/h	Atmosphere
1	/	/	/
2	600	20	air
3	900	20	air
4	1200	20	air
5	1500	20	air
6	1500	20	oxygen

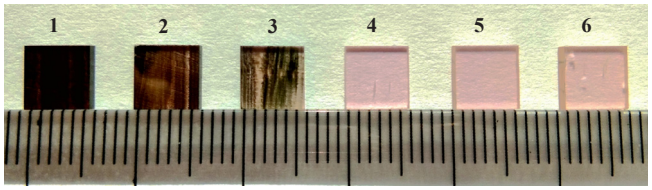

Fig. 1. The images of the Er,Yb:LuGdVO$_4$ crystal slices annealed in different conditions.

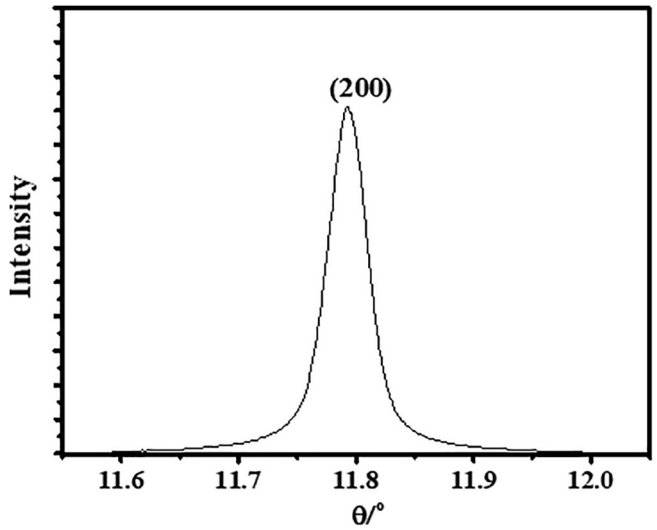

Fig. 2. X-ray rocking curve of sample1.

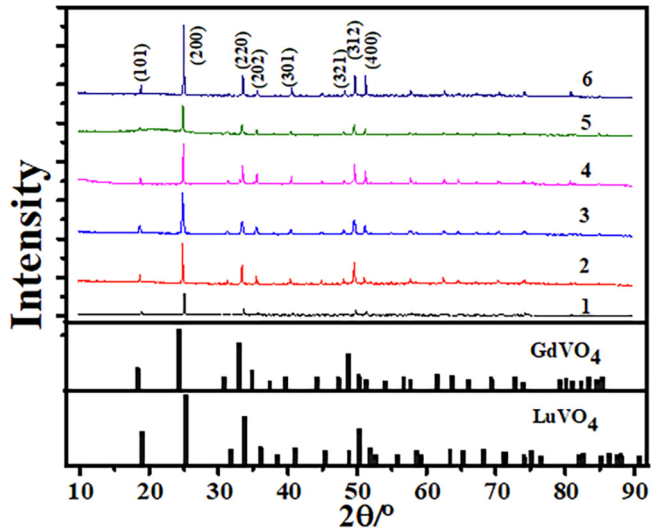

Fig. 3. The XRD patterns of the samples annealed in different conditions.

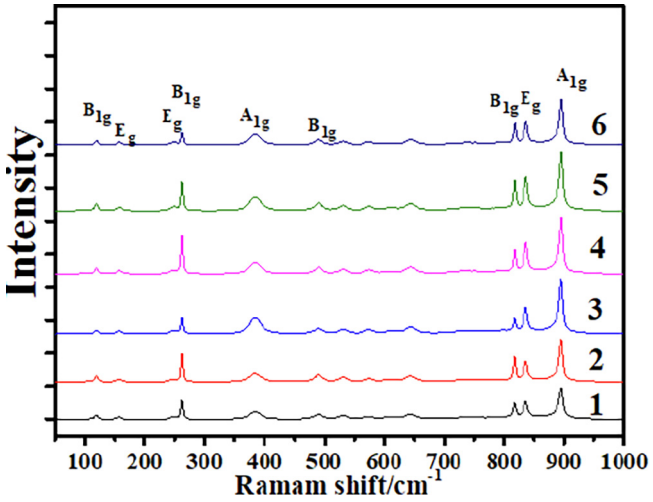

Fig. 4. The Raman spectra of the samples annealed in different conditions.

atmosphere, one black crystal was obtained, which is different from the Er^{3+} doped crystal. The crystal was cut into slices with dimensions of 6 × 6 × 2 mm^3 (a × c × b). The slices were put in to vacuum tube - furnace (GSL-1800-x), heated to 600 °C–1500 °C and maintained for 20 h in different atmospheres, then cooled down to room temperature.

The concentrations of Er^{3+} and Yb^{3+} in the Er,Yb:LuGdVO$_4$ crystal were measured by XRF analysis spectrometer (ZSX Primus II). The quality of grown crystal was characterized by high resolution X-ray diffraction (HRXRD) using the polished wafers along a-axis. The XRD patterns of samples were measured with a Bruker AXS D8 Advance diffractometer using CuKα radiation, over the 2θ range of 10°–80° at room temperature. The Raman spectra were measured using Raman microscope spectrometer (Thermo Nicolet, NEXUS 670). The XPS was performed by a spectrometer (ESCALAB250 Xi, Thermo Fisher Scientific) with a monochromatic Al Kα radiation (1486.6 eV). The polished wafers with dimensions of 6 × 6 × 2 mm^3 along a-axis direction were used for the absorption spectra measurements. The polarized absorption spectra were recorded by UV–vis-NIR spectrometer (Jasco V570) at room temperature. The X-ray absorption measurement was carried out at the beam-line 15U at Shanghai Synchrotron Radiation Facility (SSRF) for vanadium K-edge spectrum scanned from 5435 eV to 5615 eV. The absorption spectra were obtained using the - fluorescence mode. The 2D X-ray fluorescence scanning spectra were collected with the beam energy 10.5 keV at SSRF 15U beamline. The scan was run at acquisition time of 0.2 s per step and with a step size of 3 μm × 2 μm.

Results and discussions

The concentrations of Er and Yb are 0.9 mol% and 3 mol% respectively in the LuGdVO$_4$ mixed crystal, which are calculated from the XRF measurements. The crystal slices were annealed in different conditions as shown in Table 1. Sample 1 was not treated. The images of the crystal slices annealed are shown in Fig. 1. With increasing of annealing temperature, the color and transparency of the samples change obviously. After annealing at 1200 °C in the air, sample 4 turns bright pink which is consistent with the Er^{3+}, Yb^{3+} doped crystals annealed by the normal process described in Ref. [5,8]. It suggests that the common method to anneal the crystal at 1200 °C in the air is very appropriate.

The X-ray rocking curve of sample 1 is shown in Fig. 2. It is clearly that the peak is symmetrical and sharp, and the full-width at half maximum (FWHM) is 145.2″. Many dislocations and other defects were generated by oxygen-deficient atmosphere in the crystal growth, and high thermal stress was induced by the high cooling rate. All of those caused that the curve broadened, and did not result in that the crystal

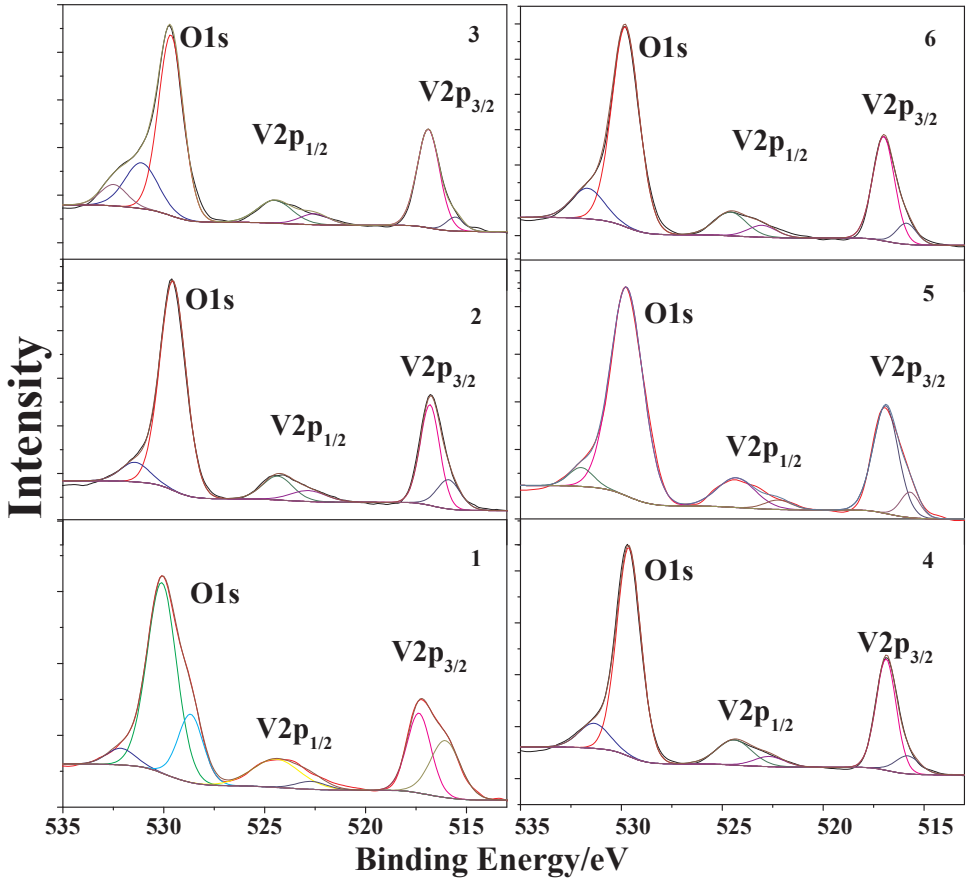

Fig. 5. XPS spectra of V2p and O1s of the samples annealed in different conditions.

Table 2
The binding energy (eV) of V.

Sample	$V^{5+}2p_{3/2}$		$V^{5+}2p_{1/2}$		$V^{4+}2p_{3/2}$		$V^{4+}2p_{1/2}$	
	BE	FWHM	BE	FWHM	BE	FWHM	BE	FWHM
1	517.4	1.44	524.4	2.89	516.0	1.83	522.7	1.83
2	516.8	1.18	524.4	2.08	515.9	1.42	522.8	1.68
3	516.9	1.36	524.5	2.11	515.6	1.08	522.5	1.78
4	516.9	1.22	524.4	2.11	515.8	1.48	522.7	1.84
5	517.0	1.53	524.4	2.31	515.9	1.42	522.6	1.62
6	517.0	1.32	524.6	1.94	515.9	1.22	522.9	1.73

cracked in the cutting process. It indicates that one relatively higher quality of crystal was obtained in the strict control of growth process.

The XRD patterns of the samples are presented in Fig. 3. It can be seen that the XRD peaks of Sample 1 is weaker, and the patterns are in accordance with the JCPDS data of $LuVO_4$ (JCPDS card No. 17-0880) and $GdVO_4$ (JCPDS card No. 17-0260). The results have confirmed that all the samples are isostructural with pure $LuVO_4$ and $GdVO_4$. The crystal structure cannot be affected under different annealing conditions, however crystallization is getting better with the increase of annealing temperature.

It has been reported that RVO_4 (R = Gd, Lu and Yb) is tetragonal zircon structure with space group $I4_1/amd$. The primitive cell contains

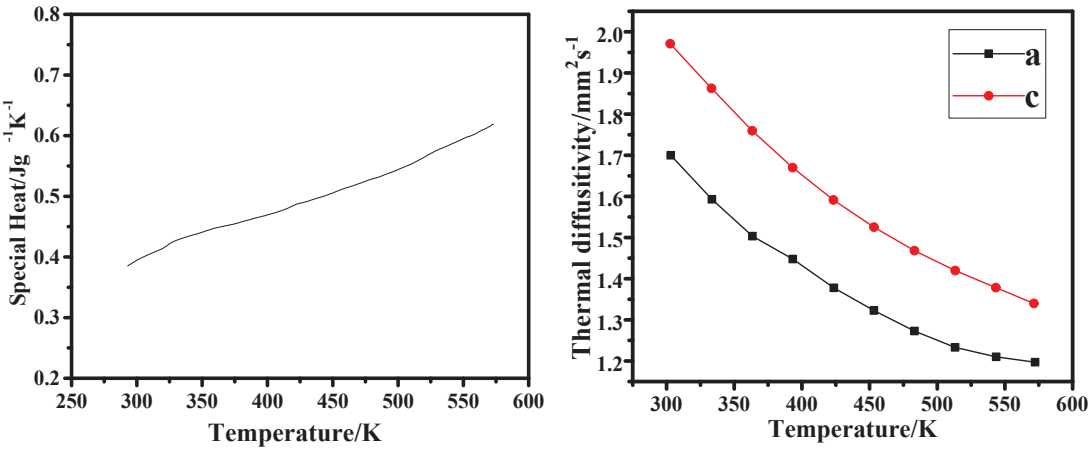

Fig. 6. The specific heat and the thermal diffusivity of sample 1.

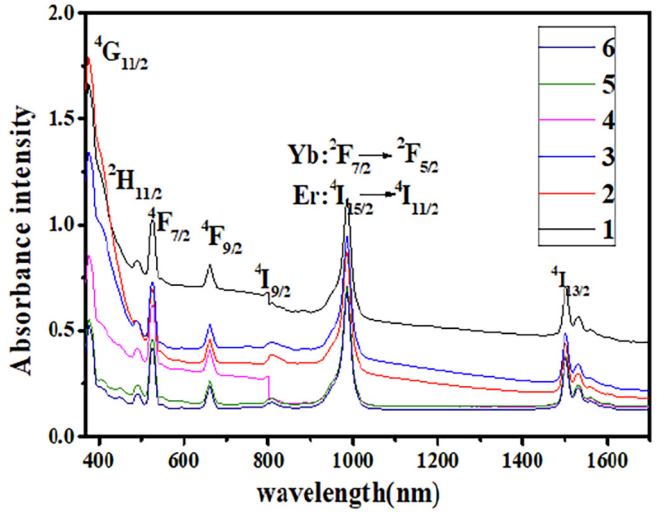

Fig. 7. The absorption spectra of the samples annealed in different conditions.

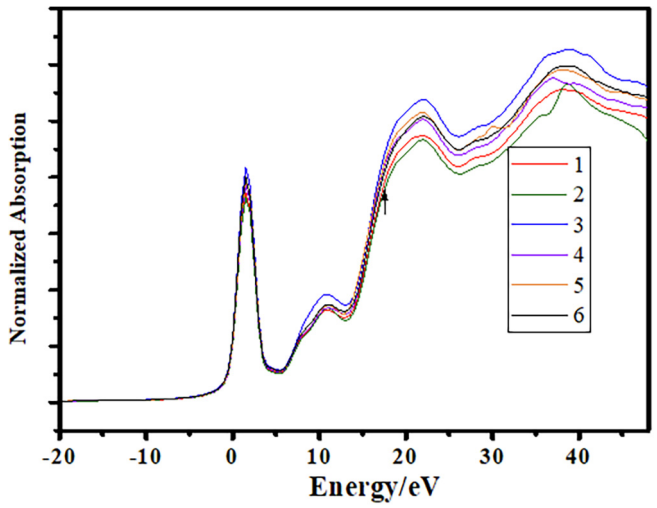

Fig. 8. Vanadium K-edge XANES spectra of the samples annealed in different conditions.

four molecular units resulting in $\Gamma = 2A_{1g} + 4B_{1g} + B_{2g} + 5E_g$ Raman active modes [9]. Fig. 4 shows that the Raman spectra of the samples are in the range of 50–1000 cm^{-1}. Nine Raman active modes are observed around 119, 157, 247, 262, 384, 498, 817, 836 and 894 cm^{-1}. The Raman active excitation frequencies of Er,Yb:$LuGdVO_4$ are close to the ones of $LuVO_4$ [10] and $GdVO_4$ [11] at room temperature. As the changes of the annealing conditions, the internal modes of the VO_4 tetrahedron and the translational or rotational motions of the Gd, Lu and VO_4 unit do not show a significant change.

The binding energies obtained in the XPS analysis are calibrated using C1s peak (284.6 eV) as a reference. It can be seen that the V 2p spectra consist of two peaks in Fig. 5. From Table 2, the V $2p_{3/2}$, V $2p_{1/2}$ peaks around 517.0 eV and 524.4 eV are attributed to V^{5+}. The binding energy of V 2p remains consistent with the relevant values of the V_2O_5 respectively [12]. The lower intensity peaks around 515.9 eV and 522.7 eV are due to V^{4+} ions. The O1s main peak at 529.7 eV is attributed to lattice oxygen O^{2-}. The shoulder peaks on the high binding energy side from 531.0 eV to 532.5 eV are attributed to adsorbed CO_2 and hydroxyl compound [13,14]. The polished surface of the crystal slice easily adsorbed CO_2 and H_2O in atmosphere. From Fig. 5-1, we can see that there are much V^{4+} ions in sample 1. And the O1s shoulder peak on the low binding energy may be assigned to O-Re, O-V^{4+}. It could be due to the severe distortion and oxygen deficiency in the lattice, the binding energy of lattice oxygen varies greatly. The oxygen ions can enter the lattices in the annealing process, but a very small amount of V^{4+} ions are still in the crystal after annealing.

The specific heat and the thermal diffusivity of sample 1 measured over the temperature range of 293–573 K are presented in Fig. 6. At room temperature, the specific heat is 0.385 $J{\cdot}g^{-1}{\cdot}K^{-1}$, and the thermal diffusion coefficients along the a- and c-axis are $\lambda_a = 1.70\ mm^2{\cdot}s^{-1}$ and $\lambda_c = 1.97\ mm^2{\cdot}s^{-1}$ respectively. The results show that thermal properties will not be affected by the atmosphere and high speed cooling rate in the growth and annealing process [15].

The π polarization (E//c) absorption spectra were recorded over the range of 350 nm–1800 nm at room temperature shown in Fig. 7. All the absorption bands are attributed to the transitions of Er^{3+} and Yb^{3+} from the ground state to different excited levels. The similar spectra can be observed for all the co-doped Er^{3+} and Yb^{3+} materials. The annealing conditions have no effect on the transitions of Er^{3+} and Yb^{3+}. The absorption of the substrate was significant decreased with the increase of the temperature. This is due to the color centers in the crystal, which are caused under the oxygen-deficient atmosphere and reduce with the increase of the oxygen atom in the lattice in different annealing conditions.

The XANES spectra can show the local symmetry, oxidation state and electronic structure of the absorbing atom in compounds [16,17]. Normalized XANES spectra for V of samples are shown in Fig. 8. The V K-absorption edge (E_0) 5465 eV should be reset to 0 eV [18]. The V K-absorption edge of samples are all about 17.6 eV, and the spectra are in good agreement with the XANES features of trivalent vanadium in NH_4VO_3 and Na_3VO_4, which is reported by Tsunehiro Tanaka [19]. The results suggest that the valence state of V is mainly pentavalent in the samples, and the lack of oxygen in the lattice has no great influence on

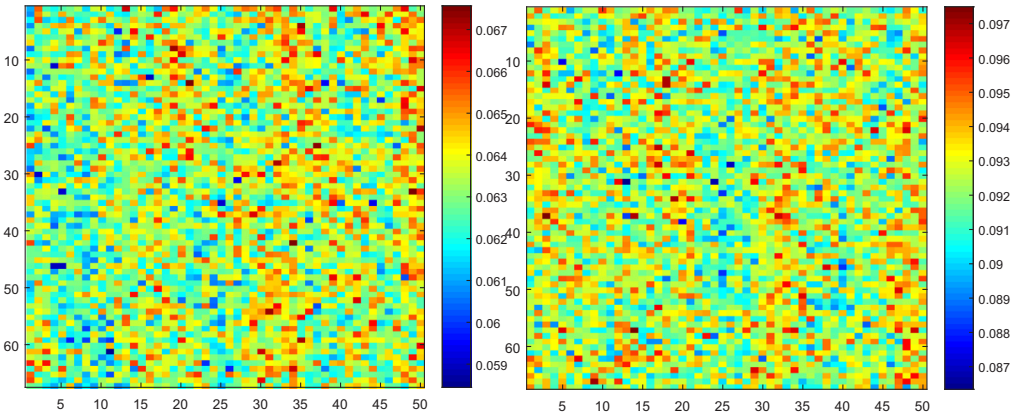

Fig. 9. SR-based XRF spectra of Lu and Gd of sample 1.

the structure of VO_4 unit.

We can see the bright and dark bands in sample 1–3. In order to explore the reasons, we presented the SR-based XRF mapping to study the distributions of Lu and Gd. Fig. 9 shows the distributions of Lu and Gd of sample 1. The 2D X-ray fluorescence scanning spectra are collected with the spot size of 4 μm × 3 μm. It can be seen that the distributions of Lu and Gd are consistent with the bands direction in the sample. That may attribute to the rapid changes of the radial gradient in the cooling process, which is resulted in the uneven distributions of the matrix elements Lu and Gd in the direction of crystal growth. However, with increasing of the annealing temperature, the bright and dark bands disappeared and the distributions of Lu and Gd became uniform, therefore the quality of the crystal were improved.

Conclusion

The Er,Yb:$LuGdVO_4$ crystal has been grown by Czochralski method under the oxygen-deficient atmosphere, then annealed under different annealing conditions. The effects of annealing conditions on the structures and properties of the samples were investigated. It was found that the oxygen-deficient atmosphere has few influences on the crystal structure, Raman shift, specific heat and thermal diffusion. The results also showed that the oxygen ions can go into lattices in the annealing process, and the valence states of V, the distribution of elements and absorption spectra of the samples were well improved with increasing of temperature and oxygen content in the annealing process.

Acknowledgement

This work was supported by the National Natural Science Foundation of China (No. 31430031, No. 51372139).

References

[1] Liu J, Mateos X, Zhang H, et al. Characteristics of a continuous-wave Yb:$GdVO_4$ laser end pumped by a high-power diode. Opt Lett 2006;31(17):2580–2.
[2] Yu H, Zhang H, Wang Z, et al. Continuous-wave laser performance of Nd:$Lu_xGd_{1-x}VO_4$ operating at 1.34 μm. Laser Phys Lett 2008;5(3):181–4.
[3] Sokolska I, Heumanna E, Kiicka S, et al. Er^{3+}:YVO_4 and Er^{3+},Yb^{3+}:YVO_4 crystals as laser materials around 1.6 μm. Adv Solid State Lasers 2001;50:378–82.
[4] Meng X, Zhu L, Zhang H, et al. Growth, morphology and laser performance of Nd:YVO_4 crystal. J Cryst Growth 1999;200(1):199–203.
[5] Xiong W, Lin S, Xie Y. Growth and spectral properties of Er^{3+}: $GdVO_4$ crystal. J Cryst Growth 2004;263(1–4):353–7.
[6] Zhang H, Meng X, Zhu L, et al. Growth and thermal properties of Nd:$GdVO_4$ single crystal. Mater Res Bull 1999;34(10–11):1589–93.
[7] Ji N, Chen Y, Li Z, et al. Characterization of $LuGdVO_3$ mixed crystal prepared by one new method. Results Phys 2019;12:335–8.
[8] Zhuang N, Hu X, Gao S, et al. Spectral properties and energy transfer of Yb, Er:GdV_O4 crystal. Appl Phys B 2006;82:607–13.
[9] Santos CC, Silva EN, Ayala AP, et al. Raman investigations of rare earth orthovanadates. J Appl Phys 2007;101(5). p. 053511-1-5.
[10] Rao R, Garg AB, Sakuntala T, et al. High pressure Raman scattering study on the phase stability of $LuVO_4$. J Solid State Chem 2009;182(7):1879–83.
[11] Harley RT, Hayes W, Smith SRP. Raman study of phase transitions in rare earth vanadates. Solid State Commun 1971;9(9):515–7.
[12] Bondarenka V, Grebinskij S, Mickevičius S, et al. Determination of vanadium valence in hydrated compounds. J Alloy Compd 2004;382(1–2):239–43.
[13] Zhang Y, He H, Zhu W, et al. $LuVO_4$:Ln^{3+} (Ln = Sm, Eu, Dy, Er and Tm) with high uniform size and morphology: controlled synthesis, growth mechanism and optical properties. CrystEngComm 2011;13(21):6471–80.
[14] Wang S, Zhao L, Bai L, et al. Enhancing photocatalytic activity of disorder-engineered C/TiO_2 and TiO_2 nanoparticles. J Mater Chem A 2014;2(20):7439–45.
[15] Ji N, Chen Y, Li Z, et al. Growth, thermal and spectral properties of Er^{3+}/Yb^{3+}:$Lu_{0.5}Gd_{0.5}VO_4$ mixed crystal. J Cryst Growth 2018;500:63–7.
[16] Liu RS, Cheng YC, Gundakaram R, et al. Crystal and electronic structures of inverse spinel-type $LiNiVO_4$. Mater Res Bull 2001;36(7):1479–86.
[17] Stöhr J. NEXAFS spectroscopy. Springer; 1992. p. XVI.
[18] Bordage A. The spectroscopic properties and electronic structure of the vanadium in complex materials: geological and technological implications. Paris VI: Université Pierre et Marie Curie; 2009.
[19] Tanaka T, Nishimura Y, Kawasaki S, et al. X-Ray absorption spectroscopy (EXAFS/XANES) evidence for the preferential formation of isolated VO_4 species on highly photoactive V_2O_5/SiO_2 catalysts. J Chem Soc Chem Commun 1987;7:506–8.